21, rue d'Artois, F-75008 PARIS
http : //www.cigre.org

CIGRE US National Committee
2015 Grid of the Future Symposium

A Wave Shape Based Algorithm for Fast CT Saturation Detection

A. RAHMATI
SunEdison
USA

SUMMARY

Operation of the protective relays depend on the secondary current of the current transformers (CT). Usually, the CT core is saturated during high through fault currents; this causes dreadful effects in the operation of protective relays. If CT enters into the saturation area the secondary current doesn't follow the primary current appropriately and may cause the mal-operation or operating time delay of the protective relays. Therefore, it is vital to identify the CT saturation effectively and compensate the disturbed current or block the relay when CT enters into the saturation area. This paper proposes an accurate solution towards detection of CT saturation problems. The proposed method describes an algorithm in which CT saturation is detected by the decomposition of even and odd set-samples of the disturbed current. The proposed method detects the CT saturation in one quarter of a power system cycle. High speed and accuracy under different saturation conditions are the main advantages of the proposed method. Various case studies were conducted using EMTP/ATP. The results are very encouraging and show that this method is able to identify all cases of CT saturation accurately.

KEYWORDS

Current transformer, decaying DC component, even samples, odd samples, saturation detection, wave-shape analysis.

arahmati@sunedison.com

Introduction

Current transformers play a key role in protection of power systems, which usually suffer from magnetic core saturation due to the large AC current amplitude and the existing decaying DC component in the fault current [1]. Core saturation is the main disadvantage of the CTs, and causes distortion of secondary currents appearing at the protective relays inputs. This leads to inaccurate phasor measurement and miss-operation of protective relays [2]. Therefore, CT saturation must be detected and resolved as quickly as possible to prevent miss-operation of the protective relays.

Many algorithms have been proposed for detecting the CT saturation. These methods are mostly based on waveform analysis, current signal harmonics, current reconstruction using unsaturated samples, CT model based reconstructions, artificial neural networks, and wavelet transform. An algorithm based on the CT model was proposed in [3]. This method detects and compensates the secondary current using the magnetizing and CT curves. A nonlinear core characteristics based on the CT parameters is required in this method. The proposed method in [4] is based on acquisition of the instantaneous current and its adjustment with magnetizing current. This method requires complicated calculations to identify the core and CT parameters. To reconstruct the secondary current reference [5] uses an artificial neural network (ANN) to learn and model the CT magnetization characteristics, and restructure the waveform based on the learned characteristics. Since, the actual CT saturation characteristics vary for different CTs, these methods are not applicable in power system protection.

Using the unsaturated portions of the secondary current is another approach used to detect and reconstruct the secondary current. A method based on variable-length samples window was proposed in [6]. This method identifies the saturation portion using second order derivative, mean and median filters, and ANN. Then, the method compensates the distorted current using the samples from the unsaturated portions. The method in [7] uses wavelet transform and a threshold criterion to identify unsaturated portion, and then applies a linear regression on the unsaturated portion to recover the distorted portion. This method requires a sufficient length of unsaturated portion. The length of unsaturated portion in severe saturations is short which does not allow the algorithm to accurately detect and reconstruct the secondary current.

The third derivative of secondary current is used to detect the CT saturation in [8]. This method compares the third difference criterion with a threshold specified by the expected maximum fault current. However, the specified threshold depends on the sampling frequency rate. For high sampling frequency rates, the threshold will be very low and the saturation detection algorithm may fail. A second derivative based approach to detect and compensate the distorted current by saturation is proposed in [9]. This algorithm uses a second difference function to detect the CT saturation. Using the second difference function and magnetizing curve, it calculates the flux to estimate the magnetizing current. The magnetizing current is added to the secondary saturated current to extract the primary current. Dependency on CT parameters and mathematical reductions are the main drawbacks to this method.

Several other approaches were proposed to detect CT saturation based on wavelet transform [10] and ANN [11]. In addition to the above methods, some specific measures are based on harmonic contents. Restraining criteria such as residual current in differential relay, mathematical morphology [12], phasor measurement based computations [13], and symmetrical components [14] have been proposed to resolve the CT saturation issue. Delayed operation and reduced sensitivity are some drawbacks to these algorithms.

Considering the shortcomings of the existing methods, an efficient algorithm for CT saturation detection is proposed in this paper. This method uses the even and odd set samples of the current signal and is based on the sinusoidal wave shape features. The saturated portions are detected using the proposed saturation detection method based on the differentiate of the even and odd set samples. Unlike most of the existing CT saturation detection algorithms, the proposed method exhibits high sensitivity in detecting deep and slight saturation.

Proposed Algorithm for CT Saturation Detection

Subtraction of the even set samples and odd set samples (SEO) of the fault current is used for CT saturation detection. This part shows that the saturation portions in the SEO wave-shape are much severe than the original fault current signal. The saturation portion in the SEO begins with the high value samples and quickly decreases to zero. In a whole saturation period the sample values remain at a very low value, almost zero. Therefore, the CT saturation detection through the SEO signal is much more effective than the original fault current signal.

The faults in power systems mostly involve a DC component superimposed on the fundamental component in one or more of the three-phase currents. In the first step, it is assumed that the fault current is a purely sinusoidal signal. Based on this assumption, the SEO signal, which is subsequently used to decaying DC removal, inspects the saturation wave-shape properties and saturation detection is introduced. Then, a new algorithm based on the SEO signal is proposed to remove the decaying DC offset. In the next step, the properties of the saturated SEO wave-shape are addressed and used in the proposed CT saturation detection algorithm.

Purely Sinusoidal Fault Current

In order to obtain the SEO signal a purely sinusoidal fault current described by:

$$i(t) = A_1 \cos(2\pi f t + \varphi_1) \qquad (1)$$

where A_1 is the amplitude, φ_1 is the phase angle, and f is the frequency of fault current. The discrete form of $i(t)$ can be written in terms of even and odd samples:

$$i(n) = i^e(n) + i^o(n)$$

$$i^e(n) = A_1 \cos\left(\frac{2\pi}{N}(2n) + \varphi_1\right)$$

$$i^o(n) = A_1 \cos\left(\frac{2\pi}{N}(2n+1) + \varphi_1\right) \qquad (2)$$

where N is the number of samples per cycle. Expanding $i^o(n)$ and subtracting the even set samples from the odd set samples yields:

$$i^{eo}(n) = 2A_1 \sin\left(\frac{\pi}{N}\right) \cos\left(\frac{2\pi}{N}(2n) + \varphi_1 - \frac{\pi}{N} + \frac{\pi}{2}\right) \qquad (3)$$

From 2 and 3, $i^o(n)$ can be rewritten in terms of $i^e(n)$ and $i^{eo}(n)$ as:

$$i^o(n) = \cos\left(\frac{2\pi}{N}\right) i^e(n) + \cos\left(\frac{2\pi}{N}\right) i^{eo}(n) \qquad (2)$$

Using 1-4, the amplitude of the fault current signal i(n), is obtained from the amplitude of the SEO signal $i^{eo}(n)$, as:

$$\frac{i^{eo}(n)}{2\sin(\frac{\pi}{N})} = A_1 \cos\left(\frac{2\pi}{N}(2n) + \varphi_1 - \frac{\pi}{N}\right)$$

$$I(n) = \frac{I^{eo}(n)}{2\sin(\frac{\pi}{N})} \quad (5)$$

Where $I(n)$ and $I^{eo}(n)$ are the estimated amplitudes of the fault current and SEO signals using the DFT method, respectively. Equations 5 show that the amplitude estimation of the fault current is procurable from the SEO signal amplitude.

Proposed Decaying DC Removal Algorithm

The fault current consists of fundamental component, decaying DC component, and harmonics. Fundamental and harmonic components can be represented as sinusoidal functions, and the decaying DC component can be represented as a decaying exponential function [15, 16, and 17]. So, the discrete fault current can be mathematically expressed as follows:

$$i(n) = i_{ac}(n\Delta t) + i_{dc}(n\Delta t)$$

$$i_{ac}(n) = \sum_{h=1}^{H} A_h \cos(2\pi f_h n\Delta t + \varphi_h)$$

$$i_{dc}(n) = A_{dc} e^{-\frac{n\Delta t}{\tau}} \quad (6)$$

where f_h, $A_h$and φ_h represent the frequency, amplitude, and phase angle of the h[th] order harmonic, and $A_{dc}$and τ are magnitude and time constant of the exponential component, respectively. H is the maximum harmonic order in the fault current. The frequency components with order more than H are eliminated by an anti-aliasing low-pass filter. The sampling frequency is $f_s = 10kHz$ and $\Delta T = 1/f_s$. The even and odd set samples of the fault current in 6 are:

$$i^e(n) = A_1 \cos\left(\frac{2\pi}{N}(2n) + \varphi_1\right) + A_o e^{-\frac{\Delta t}{\tau}(2n)}$$

$$i^o(n) = A_1 \cos\left(\frac{2\pi}{N}(2n+1) + \varphi_1\right) + A_o e^{-\frac{\Delta t}{\tau}(2n+1)} \quad (7)$$

After expanding the odd set samples in 7 and after simplifications, the following expressions are obtained:

$$i^{eo}(n) = -2A_1 \sin\left(\frac{\pi}{N}\right) \sin\left(\frac{2\pi}{N}(2n) - \frac{\pi}{N}\right) + A_o(1 - e^{-\frac{\Delta T}{\tau}}) e^{-\frac{\Delta T}{\tau}(2n)}$$

$$i^o(n) = A_o \left((e^{-\frac{\Delta T}{\tau}} - \left(1 - e^{-\frac{\Delta T}{\tau}}\right) \cos\left(\frac{\pi}{N}\right) - \cos\left(\frac{2\pi}{N}\right)\right) \cdot \ e^{-\frac{\Delta T}{\tau}(2n)} + \cos\left(\frac{\pi}{N}\right) i^{eo}(n) + \cos\left(\frac{2\pi}{N}\right) i^e(n) \quad (8)$$

where $i^{eo}(n) = i^o(n) - i^e(n)$ From 8:

$$i^o(n) - \cos\left(\frac{\pi}{N}\right) i^{eo}(n) - \cos\left(\frac{2\pi}{N}\right) i^e(n) = A_o \left(1 + \cos\left(\frac{\pi}{N}\right)\right) e^{-\frac{\Delta T}{\tau}} - \left(\cos\left(\frac{\pi}{N}\right) + \cos\left(\frac{2\pi}{N}\right)\right) e^{-\frac{\Delta T}{\tau}(2n)} \quad (9)$$

Considering $d(n) = i^o(n) - \cos\left(\frac{\pi}{N}\right) i^{eo}(n) - \cos\left(\frac{2\pi}{N}\right) i^e(n)$ and rewriting it in terms of $i^e(n)$ and $i^o(n)$ and yields:

$$d(n) = \left(1 + \cos\left(\frac{\pi}{N}\right)\right) i^{o}(n) - \left(\cos\left(\frac{\pi}{N}\right) + \cos\left(2\frac{\pi}{N}\right)\right) i^{e}(n)$$

$$\frac{d(n+1)}{d(n)} = e^{-\frac{2\Delta T}{\tau}} \qquad (10)$$

From 9 and 10, the decaying DC offset parameters are obtained as:

$$\tau = \frac{-2\Delta T}{Ln\left[\frac{d(n+1)}{d(n)}\right]}$$

$$A_o = \left[\left(1 + \cos\left(\frac{\pi}{N}\right)\right) e^{-\frac{\Delta T}{\tau}} - \left(\cos\left(\frac{\pi}{N}\right) + \cos\left(\frac{2\pi}{N}\right)\right) e^{-\frac{\Delta T}{\tau}(2n)}\right]^{-1} d(n)$$

$$i_{dc}(n) = A_o e^{-\frac{\Delta T}{\tau}n}$$

$$i_{dc}^{eo}(n) = A_o\left(1 - e^{-\frac{\Delta T}{\tau}}\right) e^{-\frac{\Delta T}{\tau}(2n)} \qquad (11)$$

Where $i_{dc}(n)$ and $i_{dc}^{eo}(n)$ are the decaying DC components of the fault current and SEO signals. Therefore, the accurate fundamental frequency components of the fault current and SEO signal are obtained as:

$$i_{ac}(n) = i(n) - i_{dc}(n)$$

$$i_{ac}^{eo}(n) = i^{eo}(n) - i_{dc}^{eo}(n) \qquad (12)$$

In developing the proposed method, no any specific assumptions or approximations were made. The method can extract the fundamental frequency by using only four samples. The fast response is specifically vital for high speed protective relays. The effectiveness of the proposed method in different conditions such as noise and harmonics is investigated in the performance evaluation.

To observe the estimated decaying DC offset and fundamental component by the proposed method, the fault current test is described by:

$$i(n) = i_{ac}(n) + i_{dc}(n) = 1.5e^{-\frac{n\Delta T}{0.02}} + \cos\left(\frac{2\pi}{N}n\right) \qquad (13)$$

Both the actual and the estimated decaying DC offset are shown in figure 1. It can be seen that the proposed algorithm accurately estimates the decaying DC offset. The percentage error for the estimated decaying DC component is defined as:

$$E(n) = \frac{i_{dc}(n) - i_{dc}^{est}(n)}{i_{dc}(n)} \times 100\% \qquad (14)$$

Where $i_{dc}^{est}(n)$ and $i_{dc}(n)$ are the estimated and actual values of the decaying DC component. figure 2 shows the error, $E(n)$, for the fault current signal test in (13). As shown in this figure, the error is almost uniform with a value of 7.55%.

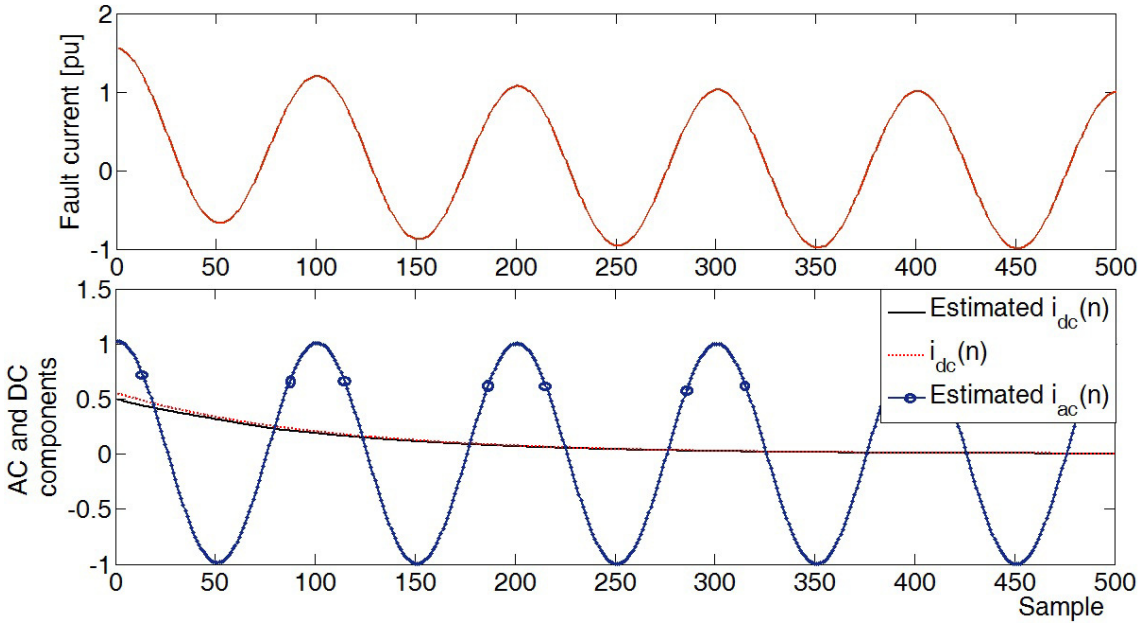

Figure 1: Extraction of the ac and dc components in the test signal

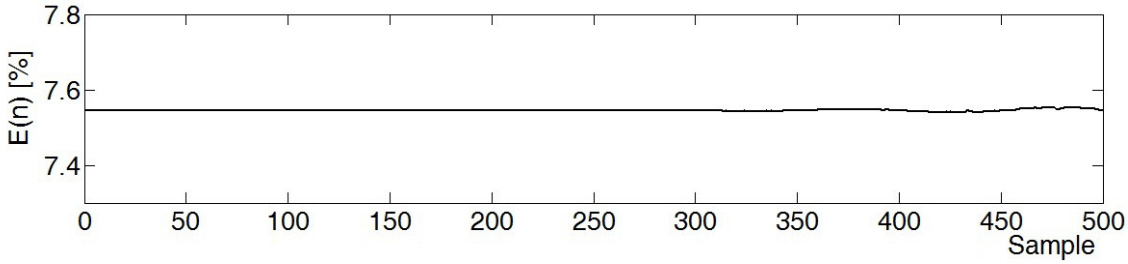

Figure 2: Error estimation of the decaying dc component

CT Saturation Detection

A distorted CT secondary current signal due to saturation contains two saturated and unsaturated distinguished portions within each cycle. As it is shown in figure 3, the current waveform is not saturated for at least 1/6 cycle (T_{u1}) before the first saturated portion (T_{S1}), and about 1/4 cycle between any two successive saturated portions (T_{u2}) [18]. As seen in figure 3, the saturated portion of the fault current signal T_S, begins with a high slope at the end of any $T_{ui}$and then its slope decrease to a low value during the saturation period. The proposed SEO signal for the same saturated fault current is shown in figure 4. It is obvious from this figure that the SEO signal slope at both the beginning and end of any saturated period T_S, is high. Moreover, the signal value at the beginning of any T_S is much higher than the rest of the saturated period. Considering (11) and a comparison of figures 3 and 4 show that the saturated fault current includes 100% of the decaying DC initial amplitude A_o. However, this value in the SEO signal is $A_o(1 - e^{-\frac{\Delta T}{\tau}})$ which is much lower than the decaying DC component in the fault current signal:

$$\frac{i_{dc}^{est}(n)}{i_{dc}(n)} = 1 - e^{-\frac{\Delta T}{\tau}} \qquad (15)$$

The existing decaying DC component in the SEO signal is very low. This component is completely removed using (12).

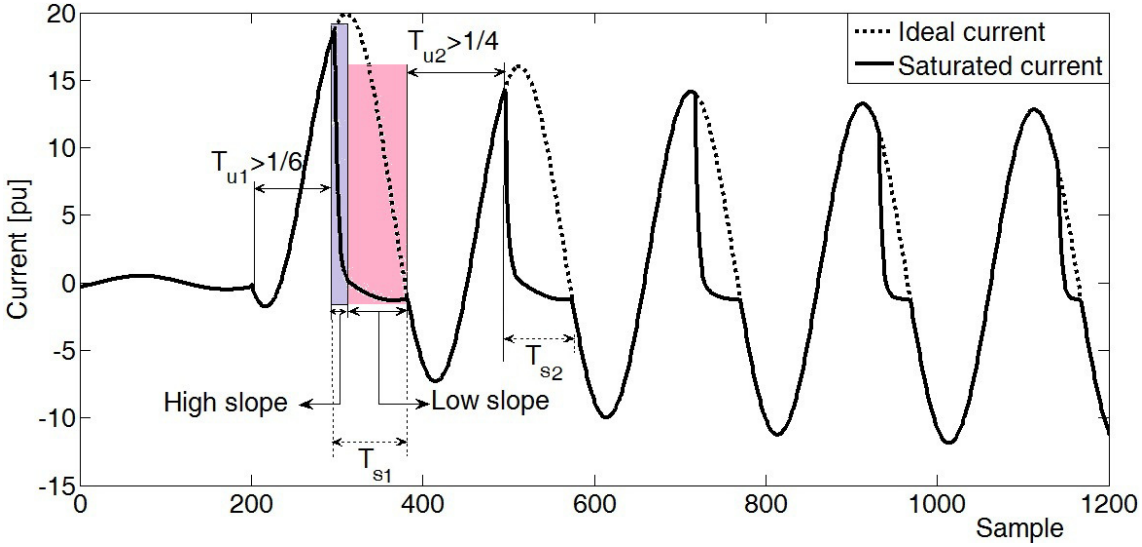

Figure 3: Distorted fault current due to CT saturation

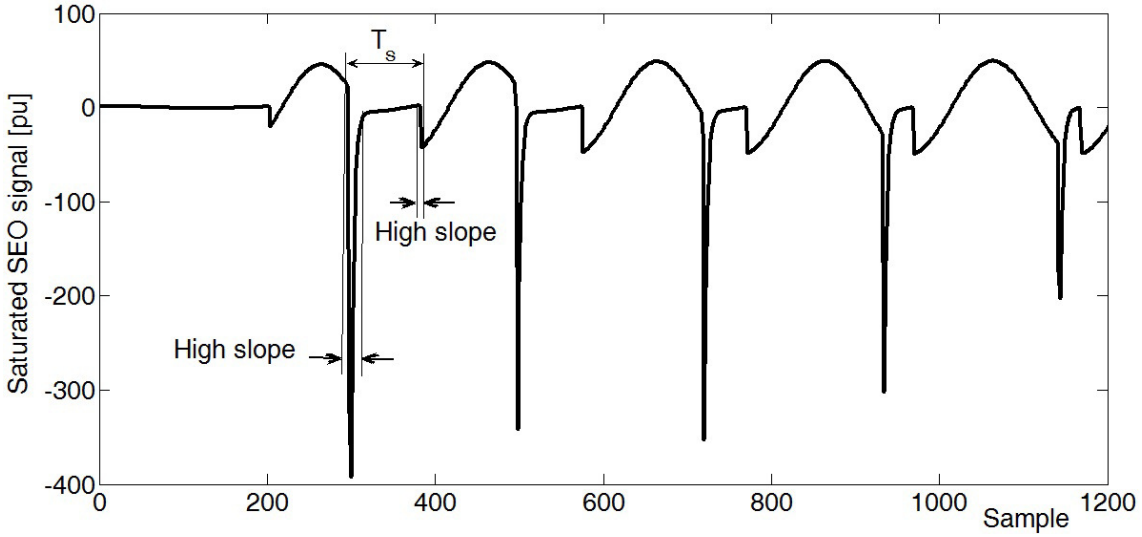

Figure 4: Distorted SEO signal due to CT saturation

Results of Simulation

To evaluate the proposed algorithm a portion of a 230 kV, 50Hz power system, shown in figure 5, is modeled appropriately using the ATP/EMTP. It includes components such as voltage source, transmission line, circuit breaker, and saturable CTs. The transmission line is 100 km and is simulated using the JMarti model [19]. The positive and zero sequence impedances of the voltage source and transmission line are $Z_+^S = 0.34 + 5.44j\ \Omega$, $Z_0^S = 2.6 + 10.12j\ \Omega$, $Z_+^L = 1.12 + 9.11j\ \Omega$, and $Z_0^L = 3.92 + 26.7j\ \Omega$, respectively. Saturable CT class is 5P20, 20 VA, and $R_{CT} = 1.5\Omega$. Two different three-phase fault were assumed occurring at 10 km and 80 km away from the CTs, and the fault resistance is $0.01\ \Omega$. The fault currents were measured by CTs with burdens $0.5\ \Omega$ and $1\ \Omega$, respectively.

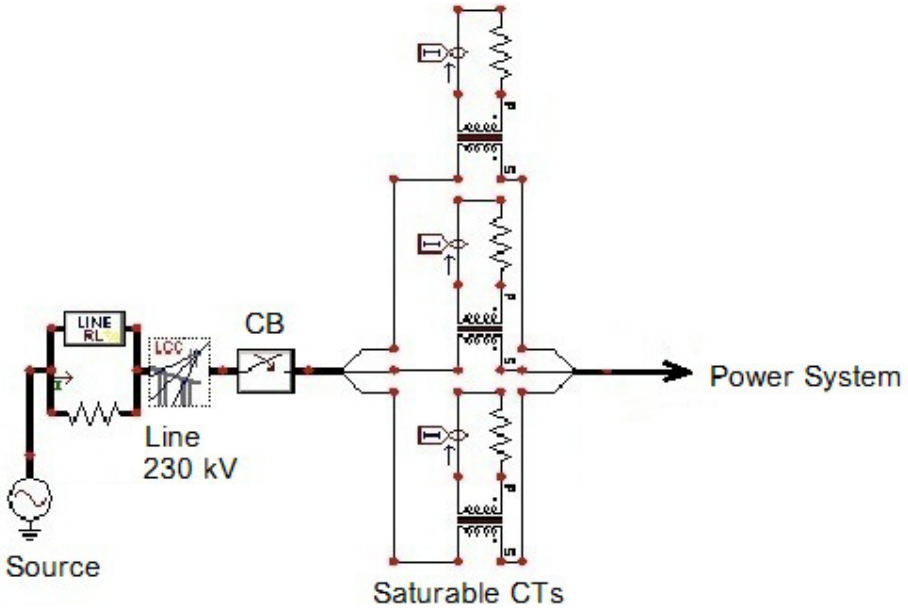

Figure 5: Simulated power system model.

Slight Saturation, CT burden $= 0.5\ \Omega$

Figure 6(a) shows the fault current in phase B for the case of slight CT saturation due to a three phase fault at $t = 0.02s$. The CT burden is $0.5\ \Omega$ in this case. The SEO signal is shown in figure 6(b).

Deep Saturation with CT burden $= 1\ \Omega$

Figure 7 shows the results for a deep CT saturation case. In this case, the CT burden is $1\ \Omega$. As figures 6(b) and 7(b) show the saturated portions (T_S) start with a sharp and high amplitude pulse. Therefore, the SEO signal is a sinusoidal signal without any decaying DC offset, which includes some pulses in saturation conditions. These pulses are located at the beginning of CT saturation area during each cycle. Therefore, using the SEO signal, and sensing its pulses, any CT saturation can be detected.

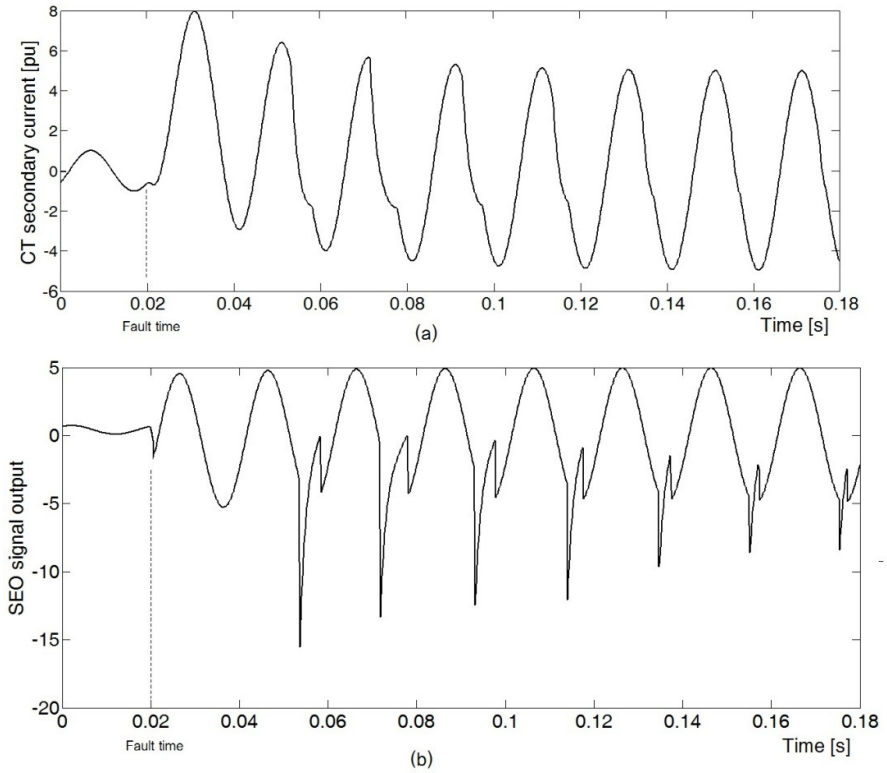

Figure 6: Slight CT saturation, (a): saturated fault currents (b): SEO signal for saturation detection

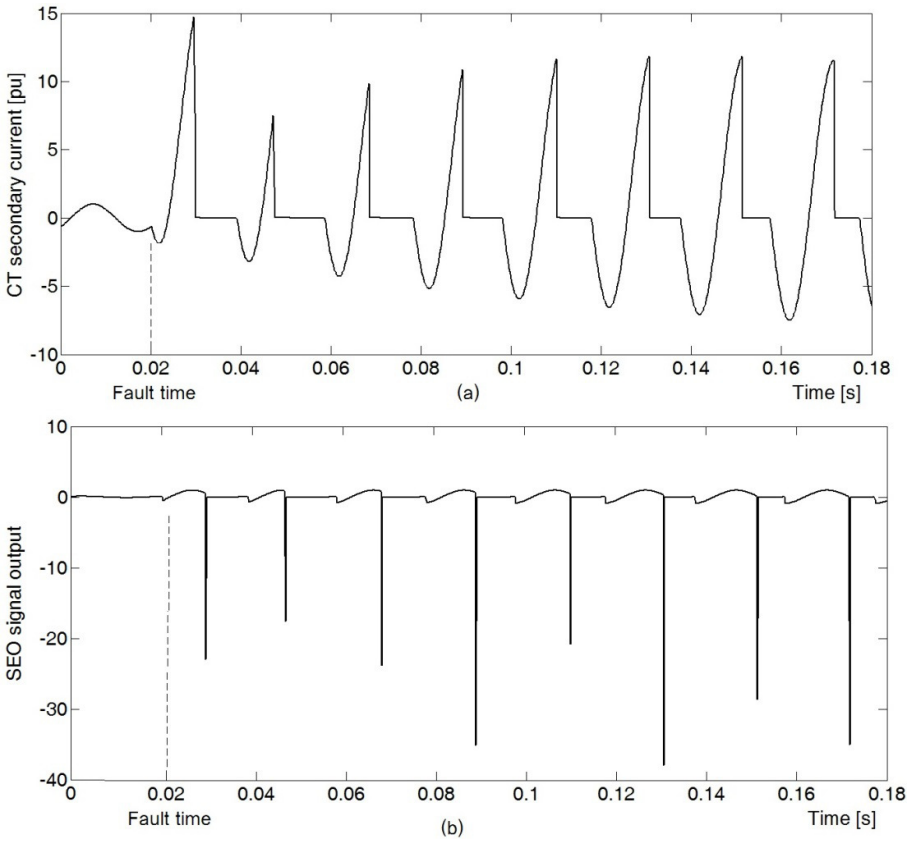

Figure 7: Deep CT saturation, (a): saturated fault currents (b): SEO signal for saturation detection

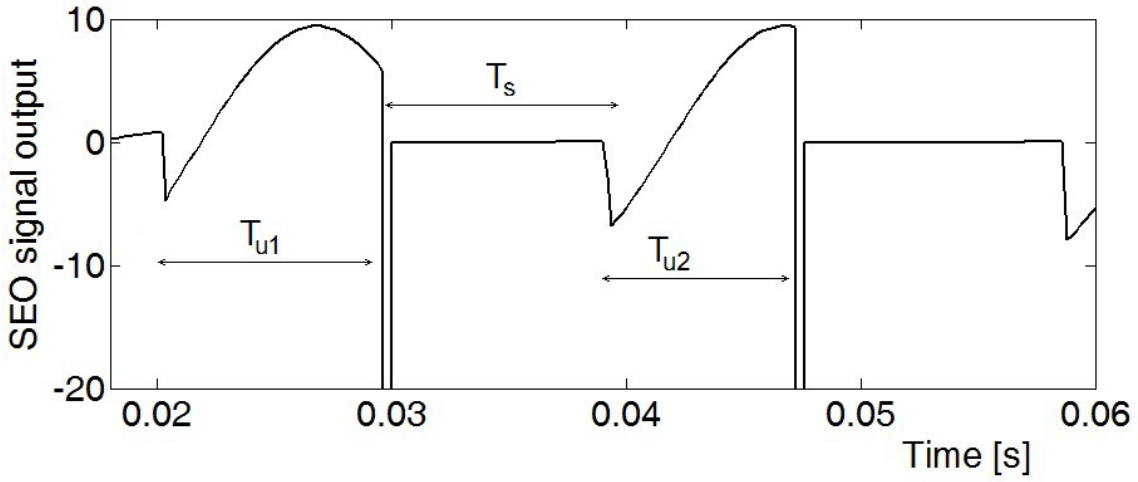

Figure 8: Expanded view of the SEO signal in deep CT saturation case

Conclusion

An efficient method for CT saturation detection was described in this paper. The proposed method is based on subtracting the even and odd set samples (SEO) of the distorted fault current. Since the decaying DC offset is completely removed from the SEO signal, the wave-shape of this signal is sinusoidal except in the saturation areas. These saturation areas start with high amplitude pulses, which easily detect the CT saturation. This method is not affected by fault conditions, such as fault type, and decaying DC characteristics, and responds quickly before CT saturation causes relay miss-operation. Moreover, it is able to detect both deep and slight CT saturation.

References

[1] Gangadharan P, Sidhu T, Klimek A. Inuence of current transformer saturation on line current differential protection algorithms. Generation, Transmission Distribution, IET 2007; 1(2):270{7. doi:10.1049/iet-gtd:20060138.

[2] Badrkhani Ajaei F, Sanaye-Pasand M, Davarpanah M, Rezaei-Zare A, Iravani R. Compensation of the current-transformer saturation effects for digital relays. Power Delivery, IEEE Transactions on 2011;26(4):2531{40. doi:10.1109/TPWRD.2011.2161622.

[3] Kang YC, Park J, Kang S, Johns A, Aggarwal R. An algorithm for compensating secondary currents of current transformers. Power Engineering Review, IEEE 1997;17(1):42{doi: 10.1109/MPER.1997.560670.

[4] Locci N, Muscas C. A digital compensation method for improving current transformer accuracy. Power Delivery, IEEE Transactions on 2000;15(4):1104{9. doi:10.1109/61.891489.

[5] Yu D, Cummins J, Wang Z, Yoon HJ, Kojovic L. Correction of current transformer distorted secondary currents due to saturation using artificial neural networks. Power Delivery, IEEE Transactions on 2001;16(2):189{94. doi:10.1109/61.915481.

[6] Kasztenny B, Rosolowski E, Lukowicz M, Izykowski J. Current related relaying algorithms immune to saturation of current transformers. In: Developments in Power System Protection, Sixth International Conference on (Conf. Publ. No. 434). 1997, p. 365{8. doi:10.1049/cp:19970100.

[7] Li F, Li Y, Aggarwal R. Combined wavelet transform and regression technique for secondary current compensation of current transformers. Generation, Transmission and Distribution, IEE Proceedings 2002;149(4):497{503. doi:10.1049/ip-gtd:20020296.

[8] Kang YC, Ok SH, Kang SH. A CT saturation detection algorithm. Power Delivery, IEEE Transactions on 2004;19(1):78{85. doi:10.1109/TPWRD.2003.820200.

[9] Kang YC, Lim UJ, Kang SH, Crossley P. Compensation of the distortion in the secondary current caused by saturation and remanence in a ct. Power Delivery, IEEE Transactions on 2004;19(4):1642{9. doi:10.1109/TPWRD.2004.835266.

[10] Hong YY, Wei DW. Compensation of distorted secondary current caused by saturation and remanence in a current transformer. Power Delivery, IEEE Transactions on 2010;25(1):47{54. doi: 10.1109/TPWRD.2009.2034820.

[11] Erenturk K. Anfis-based compensation algorithm for current-transformer saturation effects. Power Delivery, IEEE Transactions on 2009;24(1):195{201. doi:10.1109/TPWRD.2008.2005882.

[12] Lu Z, Smith JS, Wu Q. Morphological lifting scheme for current transformer saturation detection and compensation. Circuits and Systems I: Regular Papers, IEEE Transactions on 2008; 55(10):3349{57. doi:10.1109/TCSI.2008.924112.

[13] Yu CS. Detection and correction of saturated current transformer measurements using decaying dc components. Power Delivery, IEEE Transactions on 2010; 25(3): 1340{7. doi:10.1109/TPWRD.2010.2045137.

[14] Villamagna N, Crossley P. A CT saturation detection algorithm using symmetrical components for current differential protection. Power Delivery, IEEE Transactions on 2006;21(1):38{45. doi: 10.1109/TPWRD.2005.848654.

[15] Yu CS. A reiterative DFT to damp decaying dc and subsynchronous frequency components in fault current. Power Delivery, IEEE Transactions on 2006;21(4):1862{70. doi:10.1109/TPWRD.2006.877082.

[16] Mai RK, Fu L, Dong ZY, Kirby B, Bo ZQ. An adaptive dynamic phasor estimator considering dc offset for PMU applications. Power Delivery, IEEE Transactions on 2011;26(3):1744{54. doi: 10.1109/TPWRD.2011.2119334.

[17] Kang SH, Lee DG, Nam SR, Crossley P, Kang YC. Fourier transform-based modified phasor estimation method immune to the effect of the dc offsets. Power Delivery, IEEE Transactions on 2009;24(3):1104{11. doi:10.1109/TPWRD.2009.2014032.

[18] Pan J, Vu K, Hu Y. An efficient compensation algorithm for current transformer saturation effects. Power Delivery, IEEE Transactions on 2004; 19(4):1623{8.doi:10.1109/TPWRD. 2004.835273.

[19] W. Scott Meyer ThL. Electromagnetic transient program theory book. In: Bonneville power administration, Portland, Oregon. 1987.